Hydrodynamic aspects of the amorphous alloy ribbon fabrication

M. Imaizumi and M. A. Tenan

Citation: Journal of Applied Physics **65**, 4010 (1989); doi: 10.1063/1.343322
View online: http://dx.doi.org/10.1063/1.343322
View Table of Contents: http://scitation.aip.org/content/aip/journal/jap/65/10?ver=pdfcov
Published by the AIP Publishing

Hydrodynamic aspects of the amorphous alloy ribbon fabrication

M. Imaizumi
Departamento de Física, UNESP, 17033 Bauru, SP, Brazil
M. A. Tenan
Instituto de Física, Universidade Estadual de Campinas, 13081 Campinas, SP, Brazil

(Received 7 December 1988; accepted for publication 5 January 1989)

Conditions for as-quenched amorphous ribbon fabrication by a single roll-casting method are analyzed from a hydrodynamic standpoint. The analysis is based on the investigation of the processing conditions for $Fe_{40}Ni_{40}P_{14}B_6$ amorphous ribbons. It is shown that the dependence of ribbon thickness on the ejection pressure for different roll angular velocities and different dimensions of crucible and orifice can be obtained from general considerations on the melt flow regime.

I. INTRODUCTION

In recent years the possibility of important technological applications of amorphous alloy ribbons has aroused great deal of interest,[1,2] and much attention has been focused on their formation and processing conditions.[3–6] The attempts of mathematically describing the hydrodynamic step of the fabrication process are based on the assumption that the melt is an inviscid fluid which obeys Bernoulli's equation.[5,6] However, depending on Reynolds number, energy losses in the flow through an orifice within a pipe or at its end cannot be neglected.[7–9] While the discrepancies between theory and experiment in the case of Ref. 5 could be attributed to experimental errors, the more refined treatment in Ref. 6 faced difficulties which could not be convincingly resolved. Hence the mathematical development of the melt flow deserves to be reexamined.

Reformulating the main assumption on the melt flow, we thus study in this paper the role played by hydrodynamics in amorphous ribbon fabrication. The study is based on the investigation of the processing conditions of $Fe_{40}Ni_{40}P_{14}B_6$ amorphous ribbons.[10] Our results and those of Ref. 6 are analyzed by taking into account the basic phenomena of fluid discharge through orifices.

II. EXPERIMENT

A diagram of the apparatus used in our experiment is shown in Fig. 1. It consists of a copper roll (20 cm in diameter) used as a substrate to obtain amorphous ribbons from a master alloy of nominal composition $Fe_{40}Ni_{40}P_{14}B_6$. A 1-g charge of this master alloy was precisely weighed by an electronic balance and then placed in a quartz crucible (8 mm o.d. and 7 mm i.d.) having a circular orifice (0.5 mm in diameter) at its bottom. After each run, the crucible was cleaned to maintain the original size. By doing this, the same crucible was used in each series of experiments. For all runs the distance between the orifice and the copper roll surface was held fixed at 1 mm and the quartz tube axis made a constant 10° angle with respect to the vertical direction. The melt temperature measured by an optical pyrometer was determined to be 1100 °C. All amorphous ribbons were cast in such a way that the resultant width was about 1.5 mm and the resultant thickness ranged from 15 to 30 μm. To get high-quality continuous amorphous ribbons of different thicknesses two series of runs were performed. In the first series, the gauge pressure of the gas (pure argon) above the melt was varied step by step from 1.0 to 2.5 kgf/cm^2, while keeping the roll angular velocity fixed at 3000 rpm. Conversely, in the second series, the angular velocity was changed from 2000 to 3500 rpm at a constant gauge pressure of 1.8 kgf/cm^2 [1 kilogram force (kgf) = 9.806 65 N].

In our experiment it was observed that for all runs for which the gauge pressure was greater than 2.3 kgf/cm^2 or the angular velocity of roll was less than 1800 rpm, the ribbons produced were crystalline. On the other hand, in the cases for which the gauge pressure was less than 1.0 kgf/cm^2 or the roll angular velocity was greater than 3500 rpm, the ribbons produced were amorphous but porous.

The as-quenched ribbons were examined by x-ray diffraction using Cu$K\alpha$ radiation to evaluate the nature of their amorphous structure.

III. RESULTS AND DISCUSSION

The basic equation for the melt discharge through the orifice at the bottom of the crucible can be written as[9]

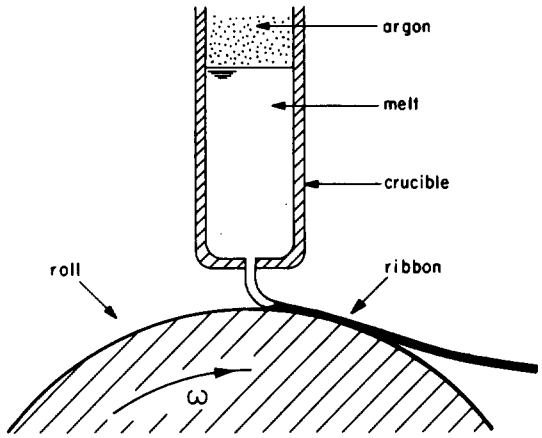

FIG. 1. Apparatus for ribbon fabrication (schematic not on scale).

 0021-8979/89/104010-04$02.40

$$Q = cA_2\sqrt{(2/\rho)\Delta p}, \tag{1}$$

where Q is the volume flow rate, c is the discharge coefficient, A_2 is the orifice area, ρ is the melt density, and Δp is the pressure drop due to melt flow through the orifice.

The dimensionless coefficient c in Eq. (1) depends primarily on (i) the ratio between the orifice area A_2 and the crucible inner cross sectional area A_1, and (ii) the Reynolds number,

$$N_R = \frac{4}{\pi}\frac{\rho}{\mu}\frac{Q}{d_1}, \tag{2}$$

for the melt flow in the crucible. In Eq. (2), μ is the melt viscosity and d_1 is the crucible inner diameter.

It is an experimental fact[8] that the discharge coefficient is much smaller than unity for very low Reynolds numbers and increases with increasing N_R until it reaches a maximum value. A further increase in the Reynolds number results in a decrease in c, and finally the coefficient becomes nearly constant for large N_R. The computed values of c for the melt discharge in our experiment when plotted together with those from Ref. 6 display this general trend (see Fig. 2).

If we combine Eq. (1) with Eq. (2), we get the relation

$$\frac{N_R}{c} = \frac{4}{\pi}\frac{\sqrt{2\rho}}{\mu}\frac{A_2}{d_1}\sqrt{\Delta p}, \tag{3}$$

which shows that for a given liquid alloy at a fixed temperature and for given values of crucible and orifice dimensions, the ratio N_R/c is determined by the pressure drop Δp. Since the discharge coefficient is a function of N_R and A_2/A_1, Eq. (3) indicates that the pressure difference Δp determines the Reynolds number and consequently the flow regime for chosen values of the melt temperature and the sizes of crucible and orifice.

For the conditions of our experiment the pressure drop Δp in Eq. (3) can be taken as the ejection pressure measured above the atmospheric pressure (gauge pressure), while for the experimental conditions given in Ref. 6 Δp can be considered as the sum of the gauge pressure with the hydrostatic pressure difference due to a melt column of height $H = 1.64$ cm and a density $\rho = 7.7$ g/cm^3. In fact, the hydrostatic pressure difference in the case of our experiment ($H = 0.70$ cm and $\rho = 7.8$ g/cm^3) is approximately three orders of magnitude smaller than the applied gauge pressure. The pressure drop across a surface with a curvature radius of about the orifice dimension is negligible for both experiments, even for a surface tension value as high as 500 dyn/cm. Finally, it can be shown that the pressure drop due to flow in the crucible gives a vanishing contribution for a melt viscosity $\mu \sim 2.25$ cP (Ref. 11) and a Reynolds number below 4000.[12]

To evaluate the flow rate Q we equate the amount of melt ejected from the orifice per unit time to that of the solid ribbon produced on the roll surface per unit time. Hence we write

$$Q = \omega r l \epsilon, \tag{4}$$

where ω and r are the angular velocity and the radius of the roll, respectively, l is the width of the ribbon, and ϵ is its thickness. In writing Eq. (4) we have assumed the equality between the densities of the amorphous solid and the liquid melt.[6]

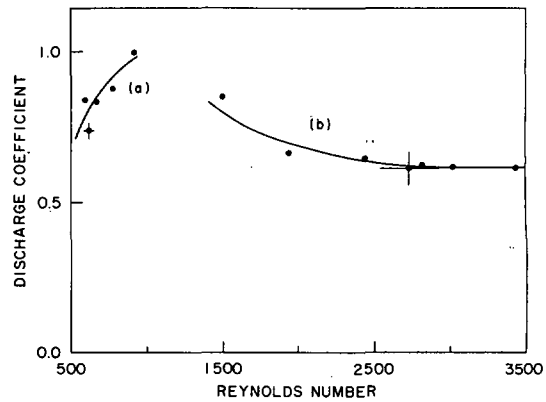

FIG. 2. Discharge coefficient as a function of Reynolds number. (a) Our experiment (area ratio: 5×10^{-3}) and (b) Ref. 6 (area ratio: 2×10^{-2}).

Figures 2 and 3 show respectively the discharge coefficient c and the ratio N_R/c as functions of the Reynolds number. The points in the figures have been evaluated from our experimental data and those of Ref. 6. To evaluate N_R we have considered Eqs. (2) and (4); the values for c have been evaluated with the help of Eqs. (1) and (4); Eq. (3) has been used for computing N_R/c. The points with bars in Figs. 2 and 3 represent average values obtained from data for different roll angular velocities at a fixed pressure drop Δp. The dispersion (rms deviation) represented by bars in the figures does not exceed 3.6% and 7.5% in the case of our experiment and of Ref. 6, respectively.

It is evident from Figs. 2 and 3 that our results and those of Ref. 6 are complementary in the sense that they concern to essentially different flow regimes as determined by Reynolds numbers below and above 2300.[12]

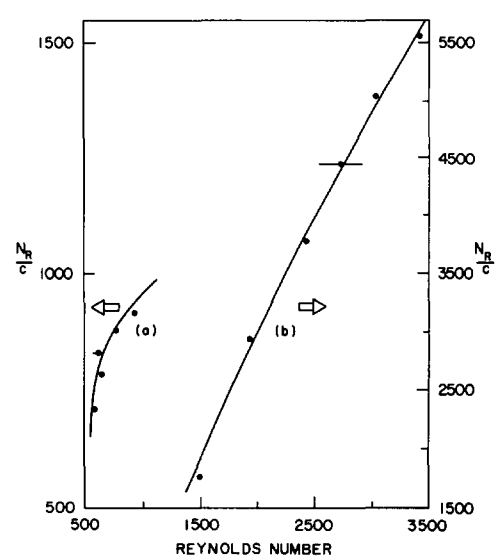

FIG. 3. Ratio N_R/c, Eq. (3), as a function of Reynolds number. (a) Our experiment and (b) Ref. 6.

As pointed out above, the pressure drop Δp determines the Reynolds number for given values of melt density and viscosity and of crucible and orifice sizes. This result implies that N_R/c vs N_R curves for different A_2/A_1 ratios play an important role in determining the conditions for amorphous ribbon fabrication: the knowledge of the quantities ρ and μ, and the choice of (i) the crucible and orifice dimensions and (ii) the pressure difference Δp will determine, via Eq. (3) and the appropriate N_R/c vs N_R curve, the corresponding Reynolds number. Since the ribbon width is essentially controlled by the orifice size,[5] the values of N_R, l (for a given orifice area A_2), and the roll radius r will be sufficient in predicting through Eqs. (2) and (4) the ribbon thickness for each value of the roll angular velocity. This procedure has been adopted in obtaining Figs. 4 and 5 from the curves in Fig. 3 and the other experimental data.

The diagrams in Figs. 4 and 5 show the predicted ribbon thickness as a function of gauge pressure for different roll angular velocities. The dashed horizontal lines in the figures represent the limits of thickness at which an amorphous ribbon can be cast continuously without porousness. The limits have been taken empirically as being $15\,\mu\text{m} < \epsilon < 35\,\mu\text{m}$ in the case of our experiment and $20\,\mu\text{m} < \epsilon < 60\,\mu\text{m}$ in the case of Ref. 6.

For comparison, experimental points for a fixed roll angular velocity are also shown in Figs. 4 and 5. In all the cases the discrepancies between experimental and predicted thicknesses do not exceed $2\,\mu$m, a value not too far from the $\pm$ 1-μm variation of thickness measured along ribbons. Hence, diagrams like those in Figs. 4 and 5 will be very helpful in determining the conditions for casting amorphous ribbons with desired thickness and width.

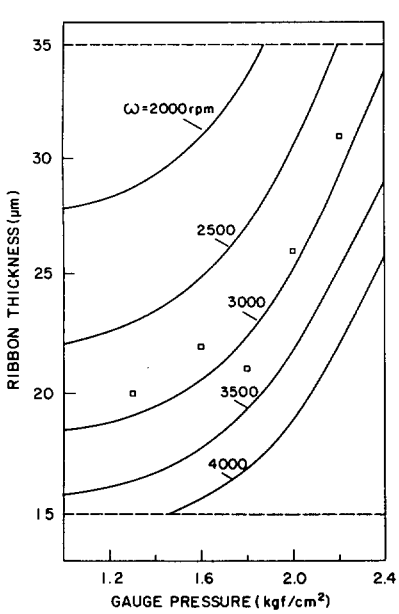

FIG. 4. Ribbon thickness as a function of the ejection gauge pressure for different values of the roll angular velocity ω. The symbols □ represent our experimental data for $\omega = 3000$ rpm.

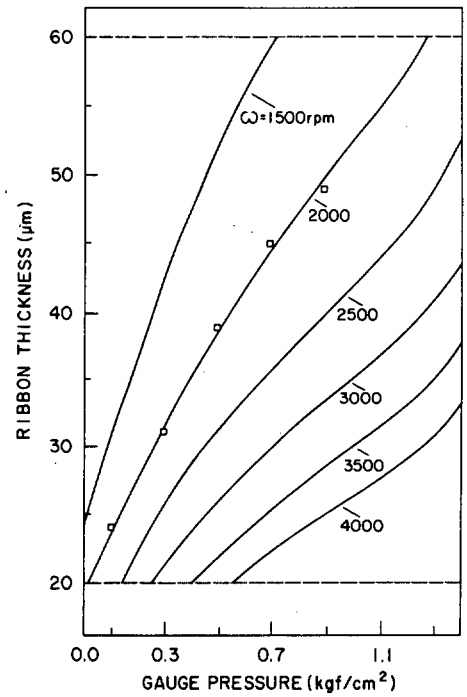

FIG. 5. Ribbon thickness as a function of the ejection gauge pressure for different values of the roll angular velocity ω. The symbols □ represent the experimental data of Ref. 6 for $\omega = 2000$ rpm.

IV. CONCLUSION

The basic outcome of the analysis presented here is that the flow regime of the melt in the crucible plays a fundamental role in determining the conditions for ribbon fabrication by the single roll-casting method. As we have seen, the knowledge of general curves of the ratio N_R/c vs N_R, for different orifice/crucible area ratios, allows us to obtain the ribbon thickness from diagrams of thickness versus gauge pressure for a given choice of the parameters which determine the flow regime.

We believe that our analysis would be useful to design new apparatuses which might optimize the processing conditions for fabrication of amorphous ribbons with prescribed dimensions.

ACKNOWLEDGMENTS

We would like to thank Dr. M. Shukla, Dr. S. Gama, and Dr. B. Laks for critically reading the manuscript. One of us (M.I.) also wishes to thank Dr. R. S. Turtelli for assistance with the experimental work.

[1]D. Raskin and C. H. Smith, in *Amorphous Metallic Alloys*, edited by F. E. Luborsky (Butterworths, London, 1983), Chap. 20; T. Hosokawa, T. Sasaki, and H. Nose, IEEE Trans. Magn. **MAG-23**, 316 (1987) (abstract); K. Kakuno, Y. Ohshima and T. Yamada, IEEE Trans. Magn. **MAG-23**, 316 (1987) (abstract); H. J. de Wit, C. H. M. Witmer, and F. W. A. Dirne, IEEE Trans. Magn. **MAG-23**, 2123 (1987); A. T. Rezende, R. S. Turtelli, and F. P. Missell, IEEE Trans. Magn. **MAG-23**, 2128 (1987); Y.-H. Lee, IEEE Trans. Magn. **MAG-23**, 2131 (1987); A. Mitra

Ghemawat, M. E. McHenry and R. C. O'Handley, J. Appl. Phys. **63**, 3388 (1988); R. Montes de Oca, E. Amano, and R. Valenzuela, J. Appl. Phys. **63**, 3391 (1988).
[2]H. Fukunaga, K. Ihara, and K. Narita, IEEE Trans. Magn. **MAG-23**, 315 (1987) (abstract); H. Yamamoto, M. Nagakura, M. Saito, and T. Miyauchi, IEEE Trans. Magn. **MAG-23**, 316 (1987) (abstract); Guo-Hau Tu, Z. Altounian, D. H. Ryan, and J. O. Ström-Olsen, J. Appl. Phys. **63**, 3330 (1988).
[3]D. R. Uhlmann, J. Non-Cryst. Solids **7**, 337 (1972).
[4]P. H. Shingu and R. Ozaki, Metall. Trans. A **6**, 33 (1975).
[5]H. H. Liebermann and C. D. Graham, Jr., IEEE Trans. Magn. **MAG-12**, 921 (1976).
[6]S. Takayama and T. Oi, J. Appl. Phys. **50**, 4962 (1979).
[7]J. C. Hunsaker and B. G. Rightmire, *Engineering Applications of Fluid Mechanics* (McGraw-Hill, New York, 1947), pp. 153–159.
[8]W. E. Howland, Trans. ASME **59**, A-53 (1937).
[9]M. P. O'Brien and R. G. Folsom, Trans. ASME **59**, 61 (1937).
[10]M. Imaizumi, M. Sc. dissertation, UNICAMP, Brasil, 1987.
[11]R. C. Weast, Ed., *CRC Handbook of Chemistry and Physics*, 62nd ed. (CRC, Boca Raton, FL, 1981), p. F-46.
[12]H. Schlichting, *Boundary-Layer Theory* (McGraw-Hill, New York, 1968), Chap. XX.